JACS
JOURNAL OF THE AMERICAN CHEMICAL SOCIETY
pubs.acs.org/JACS

Article

Nonmetal Organic Frameworks Exhibit High Proton Conductivity

Megan O'Shaughnessy, Jungwoo Lim, Joseph Glover, Alex R. Neale, Graeme M. Day, Laurence J. Hardwick,* and Andrew I. Cooper*

Cite This: J. Am. Chem. Soc. 2025, 147, 15429−15434

Read Online

ACCESS | Metrics & More | Article Recommendations | Supporting Information

ABSTRACT: Porous materials, such as metal−organic frameworks (MOFs) and porous organic salts, are promising materials for proton conduction. Recently, we developed a new subclass of porous materials, isoreticular nonmetal organic frameworks (N-MOFs), which can be designed using crystal structure prediction (CSP). Here, two porous, isostructural, and water-stable halide N-MOFs were prepared and found to show good proton conductivity of up to 1.1×10^{-1} S cm^{-1} at 70 °C and 90% relative humidity. Changing the halides in these N-MOF materials affects the resulting proton conductivity, as observed in previous studies involving MOFs and lead halides. Although this is the first study of proton conductivity in N-MOFs, the bromide salt, **TTBT.Br**, shows a higher conductivity than most polycrystalline MOFs and porous organic salts, approaching that of Nafion.

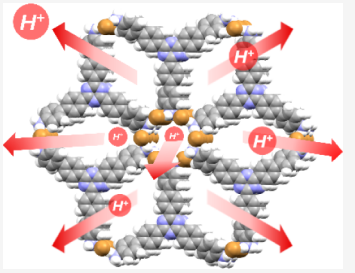

INTRODUCTION

Materials that exhibit high proton conductivity are important for the efficient conversion of chemical energy into electrical energy.[1,2] Proton-conducting materials are used in fuel cells, electrolyzers, batteries, and sensors. Hence, the development of materials with high proton conductivity is needed to move us toward a hydrogen economy.

Metal−organic frameworks (MOFs) are a promising class of materials for proton conduction because of their high surface areas and tunable structures, which allow the incorporation of various functional groups or guests in the pores.[3] Often, acid groups, such as phosphonates and sulfonates, are used to tune MOFs for proton conduction because they can act as proton transfer sites, thereby increasing performance.[4−6] Alternatively, the pores of MOFs can be loaded with molecular acids, such as H_2SO_4 and H_3PO_4, to increase proton conductivity.[7]

Porous organic salts are a related class of molecular materials that have shown promise for proton conduction.[8−11] Porous salts are produced by combining organic building blocks functionalized with acid and base groups.[12] A range of acid−base combinations has been used to form salt frameworks; not all of these exhibit permanent porosity, but this is not a hard requirement for proton conduction. One of the best-performing porous organic salts for proton conductivity was reported by Bai et al., where a guanidinium arylphosphate showed a conductivity of 4.38×10^{-2} S·cm^{-1} (90 °C, 90% relative humidity, RH).[8] Yan Teng and coworkers reported a series of porous salts in 2018: CPOS-1, which was permanently porous, showed one of the highest proton conductivities reported at that time (1.0×10^{-2} S cm^{-1}, 60 °C, 98% RH).[12] This team later incorporated H_2SO_4 into the pores of CPOS-1 to further enhance its performance to 1.4×10^{-2} S cm^{-1} (30 °C, 100% RH).[13] Another method that has been used to enhance proton conductivity in porous organic salts is to form hybrid membranes with Nafion.[14,15] Zhao et al.[16] demonstrated the effectiveness of this method when they increased the performance of iHOF-8 from 5.02×10^{-3} S cm^{-1} (100 °C, 98% RH) to 1.6×10^{-1} S cm^{-1} (100 °C, 98% RH) by using Nafion with the material to form a membrane.

Recently, we reported a series of isostructural salts (nonmetal organic frameworks, N-MOFs).[17] We showed that these materials exhibit properties that are, in many ways, like MOFs. For example, they can form isostructural families. These N-MOFs were formed using organic acids, such as hydrogen halides, whereby the halide ions are analogous to the metal nodes in MOFs. These porous molecular crystals were designed from first principles using crystal structure prediction (CSP),[18,19] which showed that the porous phases observed experimentally were the thermodynamically most stable crystal packings available.

Based on these CSP calculations, we speculated that these porous N-MOFs might have good stability for practical applications, unlike many metastable frameworks that tend to collapse and form denser, nonporous structures.[17] This was demonstrated initially for the application of iodine capture. This thermodynamic stability, coupled with the polar pore channels in these N-MOFs, prompted us to explore these materials as proton conductors.

Received: January 24, 2025
Revised: March 26, 2025
Accepted: March 27, 2025
Published: April 24, 2025

https://doi.org/10.1021/jacs.5c01336
J. Am. Chem. Soc. 2025, 147, 15429−15434

RESULTS AND DISCUSSION

Of the three NMOFs reported in our previous study,[17] **TTBT.Cl** **TTBT.Cl** (4′,4‴,4⁗′-(1,3,5-triazine-2,4,6-triyl)tris-[[1,1′-biphenyl]-4-amine] chloride) seemed most promising as a potential proton conductor because it is water stable and water insoluble, as well as being suggested by CSP to be the thermodynamically most stable structure. **TTBT.Cl** also adsorbs a substantial quantity of water (12.4 mmol g^{-1}), and water sorption has been shown to improve high proton conductivity in some materials. Here, we also prepared the bromide analogue of **TTBT.Cl**, **TTBT.Br**. We chose to study this bromide analogue because previous reports for MOFs and lead halides have shown that conductivity can be tuned by varying the halides.[20,21] CSP suggested that **TTBT.Br** would most likely crystallize like **TTBT.Cl** (Figure 1a,b). The two

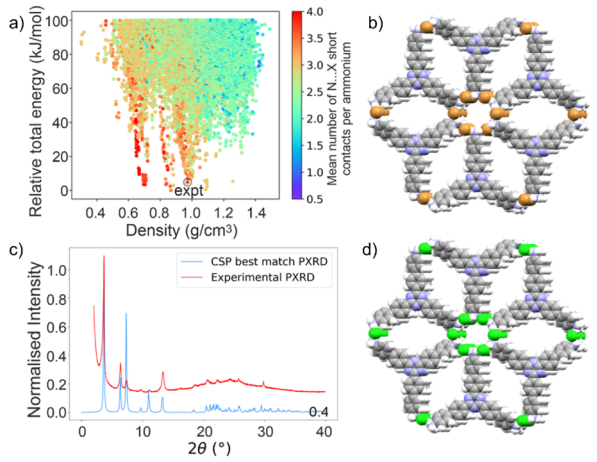

Figure 1. (a) Lattice energy landscape of predicted crystal structures for **TTBT.Br**, where each point corresponds to a distinct structure produced by CSP; data points are colored by NH_3···halide close contacts. The predicted structure corresponding to the experimental structure is labeled in the image. (b) CSP space-filling packing model for **TTBT.Br** showing 1D polar salt pore channels. (c) PXRD patterns for the experimental material and low-energy CSP structure for **TTBT.Br**. (d) CSP space-filling packing model for TTBT.Cl showing 1D polar salt pore channels.

predicted energy-structure landscapes have similar overall distributions of structures, including spikes corresponding to low-energy, porous structures that are stabilized by strong clustering of halide anions around the amine groups on TTBT. Many of the low-energy predicted crystal structures are common between the CSP landscapes of **TTBT.Cl** and **TTBT.Br** and one of the low-energy predicted structures for **TTBT.Br** being isostructural to the known crystal structure of **TTBT.Cl** (Figure 1c).

As for **TTBT.Cl**, attempts were made to grow single crystals of **TTBT.Br,** but the low solubility and rapid crystallization of this material made it hard to obtain suitable single crystals for single-crystal diffraction. The structure was therefore confirmed by comparing powder X-ray diffraction (PXRD) data with the predicted PXRD patterns obtained from CSP (Figure 1c). Based on the good agreement in peak positions in the PXRD and the agreement of CSP with experimental results in similar systems,[17] we believe that the largest uncertainty in the predicted structure is in the precise torsion angles of the biphenyl TTBT arms.[17]

While the growth of single crystals proved challenging, the synthesis of TTBT.***X*** (*X* = Cl, Br) was easily scaled, and multigram quantities of material could be produced in 30 min by simple dropwise addition of the respective HX solutions into a solution of the TTBT linker in tetrahydrofuran. This resulted in the instant precipitation of **TTBT.*X***, which was then collected by filtration. After drying the powders, they were pressed into 8 mm pellets using a pressure of 2 tons for 180 s, and their stability to water was tested using PXRD (Figure 2a,b). Both N-MOF samples showed good stability, so they were tested for their proton conduction performance. For the proton conductivity tests, **TTBT.Cl** and **TTBT.Br** were tested from 30−70 °C with relative humidity (RH) in the range of 60−90%. **TTBT.Cl** exhibits poor proton conductivity (10^{-6}–10^{-5} S cm^{-1}) under moderate-to-low humidity conditions (60% RH) (Figure 3a). However, under wetter environments, the proton conductivity (2.9×10^{-2} S cm^{-1} at 70 °C, 90% RH) is comparable to the more conductive organic salts reported so far (Table 1). The **TTBT.Br** material performs better, displaying high proton conductivities of $1.01(3) \times 10^{-1}$ S cm^{-1} at 70 °C, 90% RH. These conductivities are one to 2 orders of magnitude higher than **TTBT.Cl** as measured under the same temperature/humidity conditions. Indeed, the proton conductivity of **TTBT.Br** is close to that of Nafion 117 (7.5×10^{-2}, S/cm at 60 °C, 98% RH).[22] As such, **TTBT.Br** shows the highest proton conductivity of any polycrystalline organic salt reported to date. Cao et al.[23] recently reported a higher proton conductivity for a single crystal of a porous salt (iHOF-16; 0.388 S cm^{-1} at 80 °C, 98% RH), but this high value was measured along a single crystallographic axis rather than as a bulk measurement, as here.

The proton conductivity values for **TTBT.Br** are higher than those for equivalent polycrystalline pellets of iHOF-16 (2.11×10^{-2} S cm^{-1} at 100 °C and 98% RH). The conductivity of **TTBT.Br** is also higher than most MOFs, even those purposely tailored for their proton conductivity (Table 1). Increasing the degree of humidity significantly reduces the activation energy for proton transport in **TTBT.Cl** and **TTBT.Br** from 0.84 (9) to 0.69(1) eV and 0.67(2) to 0.33(5) eV, respectively (Figure 3b and d), highlighting that the transport mechanism is dependent on the water content in the pores,[24] as for other MOFs and salts. Gong et al. showed previously that changing the halide from Cl to Br resulted in lower performance,[20] while Levenson et al.[25] showed the opposite effect. In both of those earlier studies, it was concluded that it was the halide with the highest water uptake that gave the better proton conductivity. Our results also show that proton is sensitive to the water content in the pores. For this reason, the dry-state porosity (Figure 2a) and water uptake (Figure 2b) in both N-MOFs were quantified.[31]

TTBT.Br absorbs more CO_2 than **TTBT.Cl** in the dry state (Figure 2a). While it is hard to quantify, this might be because **TTBT.Br** has greater crystallinity. Indeed, we speculated earlier[17] that **TTBT.Cl** was partially crystalline based on its CO_2 uptake. Water isotherms were collected at 298 K for both materials (Figure 2b) and **TTBT.Br** showed a substantially higher water uptake of 17 mmol g^{-1}, compared to 12.5 mmol g^{-1} for **TTBT.Cl**, in keeping with its higher CO_2 uptake. This higher water content, coupled with greater crystallinity, could explain the higher proton conductivity of **TTBT.Br**, even without any anion effect. However, the strength of the ammonium halide salt interaction might also play a part in the conductivity performance, since Gong et al.[14] proposed

https://doi.org/10.1021/jacs.5c01336
J. Am. Chem. Soc. 2025, 147, 15429−15434

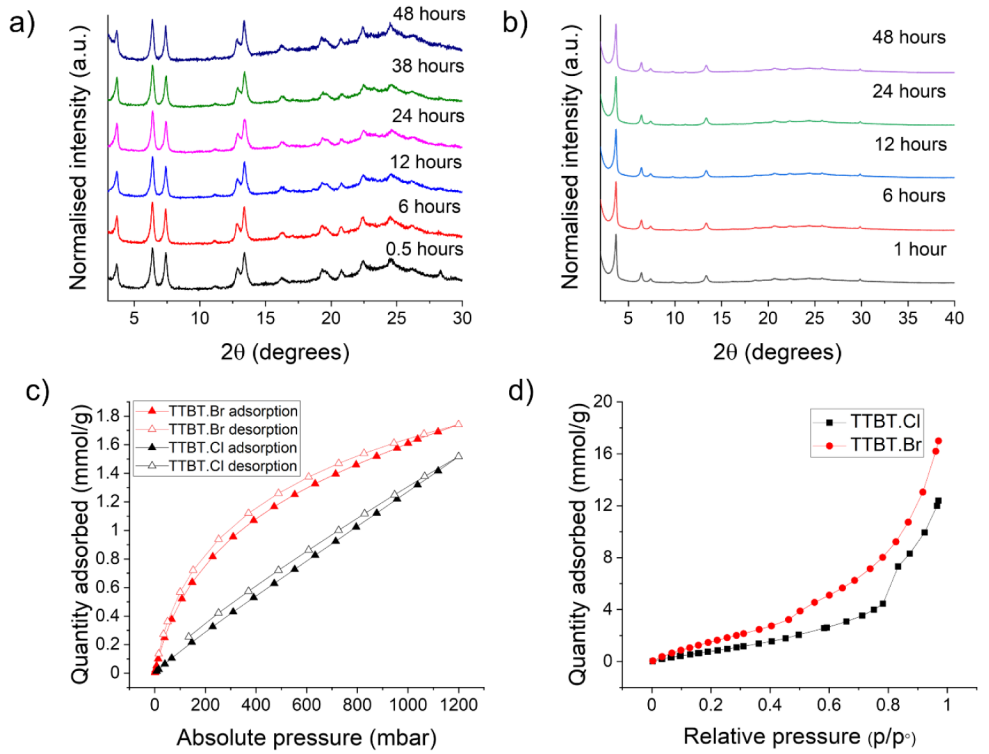

Figure 2. Stability of (a) **TTBT.Cl** and (b) **TTBT.Br** pellets over a 48 h period observed using PXRD. (c) CO_2 isotherms at 273 K for **TTBT.Cl** and **TTBT.Br,** showing their permanent porosities. (d) Water isotherms for both N-MOFs at 298 K.

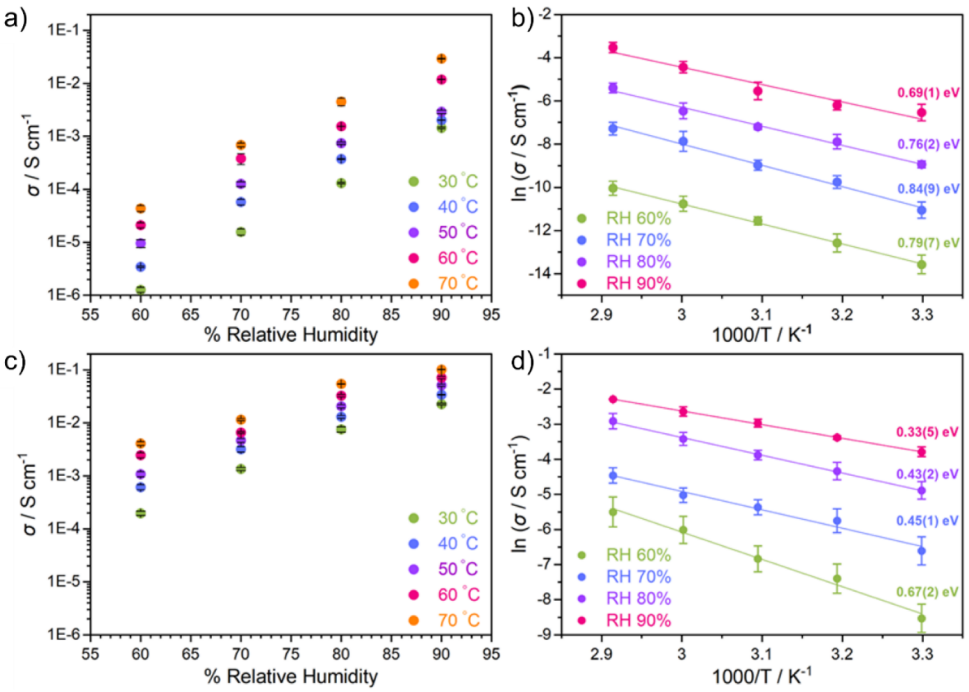

Figure 3. Proton conductivity of (a) **TTBT.Cl** and (b) **TTBT.Br** at different temperatures (30−70 °C) and humidity (60−90%), calculated based on bulk resistance from the Nyquist plot. Arrhenius plots for activation energies at different relative humidity for (c) **TTBT.Cl** and (d) **TTBT.Br**.

that chloride interactions were stronger than bromide interactions in MOFs, which boosted performance. In these N-MOFs, it is the bromide analogue, **TTBT.Br**, that has the stronger salt interaction with a ΔpK_a of 13.1, while the **TTBT.Cl** interaction is weaker (ΔpK_a of 10.7).

CONCLUSION

In conclusion, we have shown that these first-generation N-MOF materials have proton conductivity that exceeds that of other organic salts and most MOFs reported so far (Table 1). The results show that the halide counterion in the N-MOFs can modify the proton conductivity, perhaps mostly because

https://doi.org/10.1021/jacs.5c01336
J. Am. Chem. Soc. 2025, 147, 15429−15434

Table 1. The Best-Performing Polycrystalline Organic Salts and MOF Proton Conductors Reported to Date[a]

Compound	Proton conductivity (S cm^{-1})	Conditions	Reference
Organic salts			
TTBT.Br	1.1×10^{-1}	70 °C, 90% RH	This work
TTBT.Cl	2.9×10^{-2}	70 °C, 90% RH	This work
UPC-H9	2.68×10^{-2}	80 °C, 30% RH	26
CPOS-2	2.2×10^{-2}	60 °C, 98% RH	12
HOF-GS-11	1.8×10^{-2}	30 °C, 95% RH	9
TPMA-3F/MTBPS	1.34×10^{-2}	90 °C, 95% RH	27
$(C_5H_3SO_3H)(CH_2CH_2NH)$	1.18×10^{-2}	60 °C, 97% RH	28
HOF-IPCE-1Pd-NH_3	1.27×10^{-3}	85 °C, 85% RH	29
Cage salt 1	1.1×10^{-3}	30 °C, 98% RH	10
MOFs			
8HSA@MIL-101	3.06×10^{-1}	85 °C, 98% RH	24
10HSA@MOF-808-$(bSA)_2$	2.47×10^{-1}	86 °C, 98% RH	24
$[Ni(H_2O)_6][H_2tcba]$	2.1×10^{-2}	80°C, 97% RH	30
Ti-dobdc−LiI	1.26×10^{-2}	55 °C, 90% RH	21
[Zn(H2O)6][H_2tcba]	1.1×10^{-2}	80 °C, 97% RH	30
Ti-dobdc−LiCl	9.64×10^{-3}	55 °C, 90% RH	21
(UiO-66-$(SO_3H)_2$)	8.2×10^{-2}	80 °C, 90% RH	32
UiO-66-$(SO_3H)_4$	3.7×10^{-1}	90 °C, 90% RH	33
CPO-27-NCSMA	1.0×10^{-2}	60 °C, 70% RH	34
MIP-202(Zr)	1.1×10^{-2}	90 °C, 95% RH	35
PFSA polymer membrane			
Nafion 117	7.5×10^{-2}	60 °C, 98% RH	13

[a]A standard commercial grade of Nafion (Nafion-117) is included as a comparison.

the **TTBT.Br** material is more crystalline and adsorbs more water. These N-MOF materials showed reasonable stability in water and no changes in the PXRD patterns observed over several days at room temperature, which is commensurate with the predicted thermodynamic stability of these organic crystals, as anticipated by CSP. At higher temperatures, the crystallinity began to decrease slightly after 2 days. These are the first examples of N-MOF materials for proton conductivity; as such, there is significant scope to further improve their long-term stability in water and improve proton conductivity performance.

■ ASSOCIATED CONTENT

Supporting Information

The Supporting Information is available free of charge at https://pubs.acs.org/doi/10.1021/jacs.5c01336.

Materials, synthesis methods, ^{1}HNMR, IR, further proton conductivity details and computational details (PDF)

■ AUTHOR INFORMATION

Corresponding Authors

Laurence J. Hardwick − *Department of Chemistry, University of Liverpool, Liverpool L69 7ZD, United Kingdom;* orcid.org/0000-0001-8796-685X; Email: laurence.hardwick@liverpool.ac.uk

Andrew I. Cooper − *Department of Chemistry, University of Liverpool, Liverpool L69 7ZD, United Kingdom;* orcid.org/0000-0003-0201-1021; Email: aicooper@liverpool.ac.uk

Authors

Megan O'Shaughnessy − *Department of Chemistry, University of Liverpool, Liverpool L69 7ZD, United Kingdom;* orcid.org/0000-0001-6510-8344

Jungwoo Lim − *Department of Chemistry, University of Liverpool, Liverpool L69 7ZD, United Kingdom;* Present Address: LG Energy Solution, Seoul 07796, Republic of Korea; orcid.org/0000-0002-4123-2882

Joseph Glover − *Computational System Chemistry, School of Chemistry and Chemical Engineering, University of Southampton, Southampton SO17 1BJ, United Kingdom*

Alex R. Neale − *Department of Chemistry, University of Liverpool, Liverpool L69 7ZD, United Kingdom;* orcid.org/0000-0001-7675-5432

Graeme M. Day − *Computational System Chemistry, School of Chemistry and Chemical Engineering, University of Southampton, Southampton SO17 1BJ, United Kingdom;* orcid.org/0000-0001-8396-2771

Complete contact information is available at: https://pubs.acs.org/10.1021/jacs.5c01336

Author Contributions

The manuscript was written through contributions of all authors. All authors have given approval to the final version of the manuscript.

Notes

The authors declare no competing financial interest.

■ ACKNOWLEDGMENTS

AIC thanks the Royal Society for a Research Professorship (RSRP\S2\232003). The authors received funding from the Leverhulme Trust via the Leverhulme Research Centre for Functional Materials Design. This project has received funding from the European Research Council under the European Union's Horizon 2020 research and innovation program (grant agreement no. 856405). Via our membership of the UK's HEC Materials Chemistry Consortium, which is funded by the EPSRC (EP/R029431), this work used the ARCHER2 UK National Supercomputing Service (https://www.archer2.ac.uk). JL acknowledges financial support from the Faraday Institution CATMAT project (EP/S003053/1, FIRG016). MO would like to acknowledge Owen Gallagher from the Materials Innovation Factory for assistance with SEM measurements.

■ LIST OF ABBREVIATIONS

N-MOF nonmetal organic frameworks

CPOS crystalline porous organic salts
MOF metal-organic framework
CSP crystal structure prediction

REFERENCES

(1) Yoon, M.; Suh, K.; Natarajan, S.; Kim, K. Proton Conduction in Metal−Organic Frameworks and Related Modularly Built Porous Solids. *Angew. Chem., Int. Ed.* **2013**, *52*, 2688−2700.

(2) Meng, X.; Wang, H.-N.; Song, S.-Y.; Zhang, H.-J. Proton-conducting crystalline porous materials. *Chem. Soc. Rev.* **2017**, *46*, 464−480.

(3) Lim, D.-W.; Kitagawa, H. Rational strategies for proton-conductive metal−organic frameworks. *Chem. Soc. Rev.* **2021**, *50*, 6349−6368.

(4) Shimizu, G. K. H.; Vaidhyanathan, R.; Taylor, J. M. Phosphonate and sulfonate metal organic frameworks. *Chem. Soc. Rev.* **2009**, *38*, 1430−1449.

(5) Yang, F.; Xu, G.; Dou, Y.; Wang, B.; Zhang, H.; Wu, H.; Zhou, W.; Li, J.-R.; Chen, B. A flexible metal−organic framework with a high density of sulfonic acid sites for proton conduction. *Nat. Energy* **2017**, *2*, 877−883.

(6) Bao, S.-S.; Shimizu, G. K. H.; Zheng, L.-M. Proton conductive metal phosphonate frameworks. *Coord. Chem. Rev.* **2019**, *378*, 577−594.

(7) Ponomareva, V. G.; Kovalenko, K. A.; Chupakhin, A. P.; Dybtsev, D. N.; Shutova, E. S.; Fedin, V. P. Imparting High Proton Conductivity to a Metal−Organic Framework Material by Controlled Acid Impregnation. *J. Am. Chem. Soc.* **2012**, *134*, 15640−15643.

(8) Bai, X.-T.; Cao, L.-H.; Ji, C.; Zhao, F.; Chen, X.-Y.; Cao, X.-J.; Huang, M.-F. Ultra-High Proton Conductivity iHOF Based on Guanidinium Arylphosphonate for Proton Exchange Membrane Fuel Cells. *Chem. Mater.* **2023**, *35*, 3172−3180.

(9) Karmakar, A.; Illathvalappil, R.; Anothumakkool, B.; Sen, A.; Samanta, P.; Desai, A. V.; Kurungot, S.; Ghosh, S. K. Hydrogen-Bonded Organic Frameworks (HOFs): A New Class of Porous Crystalline Proton-Conducting Materials. *Angew. Chem., Int. Ed.* **2016**, *55*, 10667−10671.

(10) Liu, M.; Chen, L.; Lewis, S.; Chong, S. Y.; Little, M. A.; Hasell, T.; Aldous, I. M.; Brown, C. M.; Smith, M. W.; Morrison, C. A.; Hardwick, L. J.; Cooper, A. I. Three-dimensional protonic conductivity in porous organic cage solids. *Nat. Commun.* **2016**, *7* (1), 12750.

(11) Yang, F.-F.; Wang, X.-L.; Tian, J.; Yin, Y.; Liang, L. Vitrification-enabled enhancement of proton conductivity in hydrogen-bonded organic frameworks. *Nat. Commun.* **2024**, *15* (1), 3930.

(12) Xing, G.; Yan, T.; Das, S.; Ben, T.; Qiu, S. Synthesis of Crystalline Porous Organic Salts with High Proton Conductivity. *Angew. Chem., Int. Ed.* **2018**, *57*, 5345−5349.

(13) Wang, Y.; Yan, T.; Ben, T. Introduction of H2SO4 and H3PO4 into Crystalline Porous Organic Salts(CPOS-1) for Outstanding Proton Conductivity. *Chin. Res. Chin. Univ.* **2020**, *36*, 976−980.

(14) Bai, X.-T.; Cao, L.-H.; Chen, X.-Y.; Li, S.-H.; Zhang, J.-H. Dimethylamine-tuned guanidinium arylphosphonate iHOFs and superprotonic conduction Nafion hybrid membranes for DMFCs. *Chem. Eng. J.* **2024**, *487*, 150747.

(15) Zhao, F.; Cao, L.-H.; Bai, X.-T.; Chen, X.-Y.; Yin, Z. Application of Ionic Hydrogen-Bonded Organic Framework Materials in Hybrid Proton Exchange Membranes. *Cryst. Growth Design* **2023**, *23*, 1798−1804.

(16) Zhao, F.; Cao, L.-H.; Ji, C. Proton conduction of an ionic HOF with multiple water molecules and application as a membrane filler in direct methanol fuel cells. *J. Mater. Chem. C* **2023**, *11*, 15288−15293.

(17) O'Shaughnessy, M.; Glover, J.; Hafizi, R.; Barhi, M.; Clowes, R.; Chong, S. Y.; Argent, S. P.; Day, G. M.; Cooper, A. I. Porous isoreticular non-metal organic frameworks. *Nature* **2024**, *630*, 102−108.

(18) Jones, J. T. A.; Hasell, T.; Wu, X.; Bacsa, J.; Jelfs, K. E.; Schmidtmann, M.; Chong, S. Y.; Adams, D. J.; Trewin, A.; Schiffman, F.; Cora, F.; Slater, B.; Steiner, A.; Day, G. M.; Cooper, A. I. Modular and predictable assembly of porous organic molecular crystals. *Nature* **2011**, *474*, 367−371.

(19) Pulido, A.; Chen, L.; Kaczorowski, T.; Holden, D.; Little, M. A.; Chong, S. Y.; Slater, B. J.; McMahon, D. P.; Bonillo, B.; Stackhouse, C. J.; Stephenson, A.; Kane, C. M.; Clowes, R.; Hasell, T.; Cooper, A. I.; Day, G. M. Functional materials discovery using energy−structure−function maps. *Nature* **2017**, *543*, 657−664.

(20) Gong, L.-K.; Du, K.-Z.; Huang, X.-Y. PbX2(OOCMMIm) (X = Cl, Br): Photoluminescent organic−inorganic hybrid lead halide compounds with high proton conductivity. *Dalton Trans.* **2019**, *48*, 6690−6694.

(21) Sarango-Ramírez, M. K.; Donoshita, M.; Yoshida, Y.; Lim, D.-W.; Kitagawa, H. Cooperative Proton and Li-ion Conduction in a 2D-Layered MOF via Mechanical Insertion of Lithium Halides. *Angew. Chem., Int. Ed.* **2023**, *62*, No. e202301284.

(22) Sone, Y.; Ekdunge, P.; Simonsson, D. Proton conductivity of Nafion 117 as measured by a four-electrode AC impedance method. *J. Electrochem. Soc.* **1996**, *143*, 1254−1259.

(23) Cao, X.-J.; Cao, L.-H.; Bai, X.-T.; Hou, X.-Y.; Li, H.-Y. An Ultra-Robust and 3D Proton Transport Pathways iHOF with Single-Crystal Superprotonic Conductivity Around 0.4 S cm−1. *Adv. Funct. Mater.* **2024**, *34* (49), 2409359.

(24) Sharma, A.; Lim, J.; Lee, S.; Han, S.; Seong, J.; Baek, S. B.; Lah, M. S. Superprotonic Conductivity of MOFs Confining Zwitterionic Sulfamic Acid as Proton Source and Conducting Medium. *Angew. Chem., Int. Ed.* **2023**, *62* (29), No. e202302376.

(25) Levenson, D. A.; Zhang, J.; Szell, P. M. J.; Bryce, D. L.; Gelfand, B. S.; Huynh, R. P. S.; Fylstra, N. D.; Shimizu, G. K. H. Effects of Secondary Anions on Proton Conduction in a Flexible Cationic Phosphonate Metal−Organic Framework. *Chem. Mater.* **2020**, *32*, 679−687.

(26) Wang, Y.; Zhang, M.; Yang, Q.; Yin, J.; Liu, D.; Shang, Y.; Kang, Z.; Wang, R.; Sun, D.; Jiang, J. Single-crystal-to-single-crystal transformation and proton conductivity of three hydrogen-bonded organic frameworks. *Chem. Commun.* **2020**, *56*, 15529−15532.

(27) Ami, T.; Oka, K.; Kitajima, S.; Tohnai, N. Highly Fluorinated Nanospace in Porous Organic Salts with High Water Stability/Capability and Proton Conductivity. *Angew. Chem., Int. Ed.* **2024**, *63* (37), No. e202407484.

(28) Wei, M.-J.; Gao, Y.; Li, K.; Li, B.; Fu, J.-Q.; Zang, H.-Y.; Shao, K.-Z.; Su, Z.-M. Supramolecular hydrogen-bonded organic networks through acid−base pairs as efficient proton-conducting electrolytes. *CrystEngcomm* **2019**, *21*, 4996−5001.

(29) Zhigileva, E. A.; Enakieva, Y. Y.; Sinelshchikova, A. A.; Chernyshev, V. V.; Senchikhin, I. N.; Kovalenko, K. A.; Stenina, I. A.; Yaroslavtsev, A. B.; Gorbunova, Y. G.; Tsivadze, A. Y. An anionic porphyrinylphosphonate-based hydrogen-bonded organic framework: Optimization of proton conductivity through the exchange of counterions. *Dalton Trans.* **2023**, *52*, 8237−8246.

(30) Shao, D.; Shi, L.; Liu, G.; Yue, J.; Ming, S.; Yang, X.; Zhu, J.; Ruan, Z. Metalo Hydrogen-Bonded Organic Frameworks Self-Assembled by Charge-Assisted Synthons for Ultrahigh Proton Conduction. *Cryst. Growth Design* **2023**, *23*, 5035−5042.

(31) Park, M. J.; Downing, K. H.; Jackson, A.; Gomez, E. D.; Minor, A. M.; Cookson, D.; Weber, A. Z.; Balsara, N. P. Increased Water Retention in Polymer Electrolyte Membranes at Elevated Temperatures Assisted by Capillary Condensation. *Nano Lett.* **2007**, *7*, 3547−3552.

(32) Phang, W. J.; Jo, H.; Lee, W. R.; Song, J. H.; Yoo, K.; Kim, B.; Hong, C. S. Superprotonic Conductivity of a UiO-66 Framework Functionalized with Sulfonic Acid Groups by Facile Postsynthetic Oxidation. *Angew. Chem., Int. Ed.* **2015**, *54* (17), 5142−5146.

(33) He, Y.; Dong, J.; Liu, Z.; Li, M.-Q.; Hu, J.; Zhou, Y.; Xu, Z.; He, J. Dense Dithiolene Units on Metal−Organic Frameworks for Mercury Removal and Superprotonic Conduction. *ACS Appl. Mater. Interfaces* **2022**, *14* (1), 1070−1076.

(34) Lupa, M.; Kozyra, P.; Matoga, D. Solvent-Free Mechanochemical Dense Pore Filling Yields CPO-27/MOF-74 Metal−Organic

https://doi.org/10.1021/jacs.5c01336
J. Am. Chem. Soc. 2025, 147, 15429−15434

Frameworks with High Anhydrous and Water-Assisted Proton Conductivity. *ACS Appl. Energy Mater.* **2023**, *6* (18), 9118−9123.
(35) Wang, S.; Wahiduzzaman, M.; Davis, L.; Tissot, A.; Shepard, W.; Marrot, J.; Martineau-Corcos, C.; Hamdane, D.; Maurin, G.; Devautour-Vinot, S.; Serre, C. A robust zirconium amino acid metal-organic framework for proton conduction. *Nat. Commun.* **2018**, *9* (1), 4937.

https://doi.org/10.1021/jacs.5c01336
J. Am. Chem. Soc. 2025, 147, 15429−15434